Reproduction of Macroscopic Properties of Unsaturated Triacylglycerides using a Modified NERD Force Field

Robert J Cordina[a,b], *Beccy Smith*[b], *Tell Tuttle*[b,*]

[a] Mondelēz UK R&D Ltd., PO Box 12, Bournville Lane, Birmingham B30 2LU, UK.

[b] Department of Pure and Applied Chemistry, University of Strathclyde, 295 Cathedral Street, Glasgow G1 1XL, UK.

* tell.tuttle@strath.ac.uk +44 141 548 2290

This is a peer-reviewed, accepted author manuscript of the following article: Cordina, R. J., Smith, B., & Tuttle, T. (2021). Reproduction of macroscopic properties of unsaturated triacylglycerides using a modified NERD force field. Journal of molecular graphics & modelling, 108, [107996]. https://doi.org/10.1016/j.jmgm.2021.107996

ABSTRACT

Unsaturated triacylglycerides are found in many commonly consumed foods, such as cooking oils, nuts and chocolate. There are however very few publications on Molecular Dynamics simulations of such molecules, and, to the best of our knowledge, no such published research on crystalline mono-unsaturated triacylglycerides. The work described in this paper is an evaluation of different force fields (GROMOS96 and NERD) to determine the best force field parameters to reproduce the crystalline and melted macroscopic properties of such molecules accurately. The best results were obtained by modifying the NERD force field, through which we were able to reproduce the crystalline and melted density as well as crystal dimensions of mono-unsaturated triacylglycerides.

KEYWORDS

macroproperties; molecular dynamics; NERD; triacylglycerides; unsaturated

INTRODUCTION

There are few published studies on the Molecular Dynamics (MD) simulations of triacylglycerides (TAGs), with the main body of this work focusing on fully saturated TAGs.[1-6] The earliest work is the seminal study by Chandrasekhar and van Gunsteren,[1] where they detailed the evaluation of six GROMOS96 force field (FF) parameter sets to determine which best reproduced the properties of pure trioctanoin (a fully saturated TAG) in the gel phase, with the authors concluding that the 45A3 parameter set of this FF was the best one in this case. This work has been followed by other studies on crystalline fully saturated TAGs, such as the work by Szewczyk[2] (who used the GROMOS96 53A5 parameter set, an evolution of the 45A3 parameter set), Brasiello *et al*.[3] (who describe using the GROMOS96 FF but not the exact parameter set), and MacDougall *et al*.[4] and Razul *et al*.[5] (who use a variant of the GROMOS96 FF). A 2018 study by Pizzirusso *et al*.[6] compared the suitability of four different FFs (OPLS-AA, Large-OPLS, GROMOS96 and NERD) to reproduce the crystalline properties of tripalmitin and tristearin, with the NERD FF being shown to be the most suitable.

Unsaturated triacylglycerides (TAGs) are ubiquitous in foods, such as 1-oleoyl-2,3-dilinoeoyl-*sn*-glycerol and 1,2,3-trilinoeoyl-*sn*-glycerol in sunflower oil,[7] and 1,2,3-trioleoyl-*sn*-glycerol in hazelnuts.[8,9] Notwithstanding this, there is very little published research on the MD simulation of such TAGs, with the work by Sum *et al*.[10] and Greiner *et al*.[11] being the exceptions. However, in both these cases the TAGs are simulated in their liquid (melted/unordered) state, and not in their crystalline state. In the work by Sum *et al*.[10] the kinematic viscosity of liquid canola oil and cocoa butter were determined at different temperatures using Molecular Dynamics (MD) and a customized force field (FF) described in the same paper. Greiner *et al*.[11] used the General AMBER

FF[12] to determine the liquid density of cocoa butter, with further studies in the same publication also simulating cocoa butter in the liquid state.

Being able to simulate unsaturated crystalline TAGs accurately could be of benefit to the determination of the macroscopic properties of new crystalline TAG blends, such as those used in the confectionery industry. The confectionery industry makes use of many different fats, a number of which are interesterified, which means that their properties might not be known. Having a FF that can describe the macroscopic properties such as density and shear viscosity of such unsaturated TAGs would thus enable the industry to better predict and understand the properties of the novel fats. One of the main crystalline fats used in the confectionery industry is cocoa butter, which has been characterized extensively and shown to be made up of mostly the single unsaturated TAGs 1,3-dipalmitoyl-2-oleoyl-*sn*-glycerol (*sn*-POP), 1,3-distearoyl-2-oleoyl *sn*-glycerol (*sn*-StOSt) and 1-palmitoyl-2-oleoyl-3-stearoyl-*sn*-glycerol (*sn*-POSt),[13] which are three TAGs this study focuses on (Scheme 1).

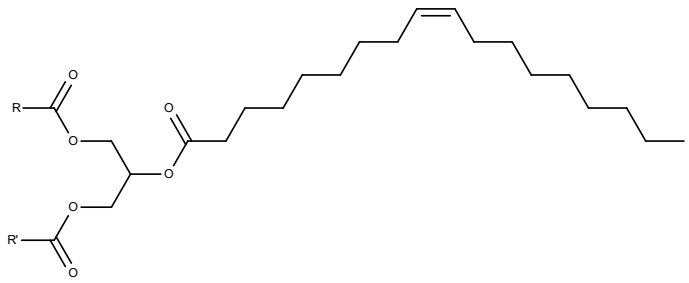

Scheme 1. General structure of unsaturated TAGs used in this study. *sn*-POP (R = R' = $C_{15}H_{31}$) *sn-StOSt* (R = R' = $C_{17}H_{35}$) *sn*-POSt (R = $C_{15}H_{31}$ R' = $C_{17}H_{35}$) *(single column image)*

All three of these TAGs are known to be polymorphic, as shown by van Mechelen *et al*.[14] and Peschar *et al*.[15] The different polymorphic forms of TAGs are termed α, β' and β, with the α form

being the least stable and β being the most stable.[16] In the case of these three TAGs the monoclinic β form has two sub-polymorphs,[14,15] the lesser-stable β_2 and the more stable β_1.

COMPUTATIONAL METHODS

All simulations were carried out using GROMACS 2019.3,[17] while all visualizations were done in VMD.[18] The GROMOS96-53A5 FF[19] was used as supplied in GROMACS 2019.3, while the NERD FF[20-22] was used as given in Sum *et al*.[10] All equilibrations were carried out using an isobaric/isothermal (NPT) ensemble, using a v-rescale thermostat and a Berendsen barostat. Constant atmospheric pressure (1.01325 bar) was maintained by using anisotropic pressure coupling, with a compressibility of $1x10^{-5}$ bar^{-1} in the *x*, *y* and *z* directions. This was done to maintain the monoclinic structure of the crystal. Temperature coupling was set at 1 ps, while pressure coupling was set at 10 ps. A time step of 2 fs was used for all equilibrations and a randomized seed was used for initializing velocities. The cut-off scheme was set to Verlet, with the Coulomb and vdW cut-off distances set to 1.1 nm, and with the vdW-modifier being set to Potential-shift. Sum *et al*.[10] describe the FF as being used with a reaction-field correction with a continuum dielectric for long-range electrostatic interactions. In this case the coulombtype was set to Reaction-Field with an epsilon-rf value of 2.975. In all other cases the coulombtype was set to Particle-Mesh Ewald (PME), while no epsilon-rf value was specified. The Potential-shift and PME settings, as well as the cut-off distances, were chosen as per Sum *et al*.'s[10] specification that interactions were cut-off and shifted by 1.1 nm, with the energies also shifted at this distance.

In all of the results below, equilibrations were carried out on a box made up of 100 molecules (25 unit cells, with each unit cell being made up of 4 molecules in the case when equilibrating crystalline structure, and 100 randomly placed molecules in the case of the melted equilibrations). The unit cells were obtained from Peschar *et al*.[15] and van Mechelen *et al*.[14] with the crystalline

box being built by stacking 5 unit cells in each of the *a* and *c* directions. Each box was minimized and equilibrated for 100 ns in the case of the crystalline boxes and 50 ns in the case of melted boxes. Where only one result is reported per setting, this is the average of triplicate equilibrations, with the results taken after equilibration had been reached.

RESULTS AND DISCUSSION

A box of β_2 *sn*-POSt was equilibrated at 250 K using the GROMOS96-53A5[19] and NERD[10] FFs with the results compared to the empirical measurements. This temperature was chosen to be the same as that at which the crystal was analyzed by X-Ray Diffraction (XRD) by Peschar *et al*.[15] Using the standard, unmodified, GROMOS and NERD FFs (*i.e*., the latter with the use of a reaction-field correction) the results obtained deviated from the empirical measurements in both cases, with the different FFs performing better or worse for different measurements (Table 1). A slightly better crystal density was obtained when using the GROMOS FF, however much larger differences in the long spacing and the angle formed by the ester oxygens (Figure 1) were observed when compared to the NERD FF (Table 1). The increase in the long spacing when using the GROMOS FF was interpreted as a relaxation of the molecular structure, leading to elongation, which is also reflected in the +9.12% difference in the *b* dimension of the crystal.

Measurements	*Empirical*[15]	*GROMOS FF*	*NERD FF*
a (Å)	27.12	25.23	24.93
b (Å)	126.53	138.06	130.25
c (Å)	40.605	40.71	44.00
α (°)	90.00	90.00	90.00

β (°)	88.51	88.62	88.73
γ (°)	90.00	90.00	90.00
Volume (Å^3)	139 336	141 792	142 872
Density (g/cm^3)	1.027	1.009	1.001
Long spacing (Å)	60.98	67.76	62.49
Glycerol backbone angle (°)	111.47	111.30	122.07
Ester oxygens angle (°)	66.65	46.91	59.17

Table 1. Comparison of empirical crystal properties of β_2 *sn*-POSt with simulated results using two different force fields

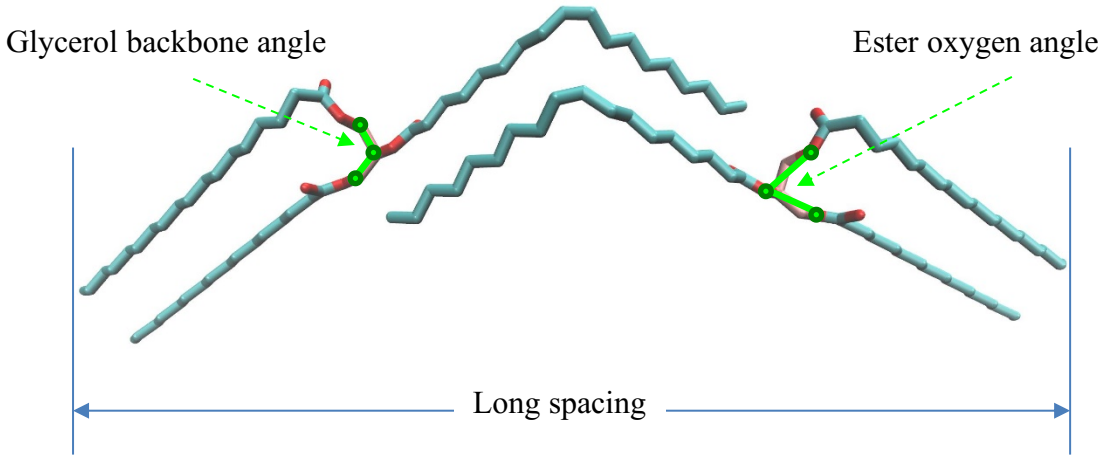

Figure 1. Definition of the measurements taken on the crystalline molecules of β_2 *sn*-POSt. *(single column image)*

On visualizing the molecules, a number of differences could be observed, both between the molecules before and after equilibration, as well as between the equilibrated molecules using the different FFs. The molecules in the crystal before equilibration are near planar, *i.e.*, the palmitic, oleic and stearic chains are on the same plane, (Figure 2a), however after equilibration the oleic

chain was found to be rotated by approximately 95° and 48° with respect to the palmitic-stearic plane when using both the GROMOS and NERD FFs respectively (Figure 2c and Figure 2e respectively – in both cases the oleic chain is visualized out of the plane while the palmitic and stearic chains are into the plane).

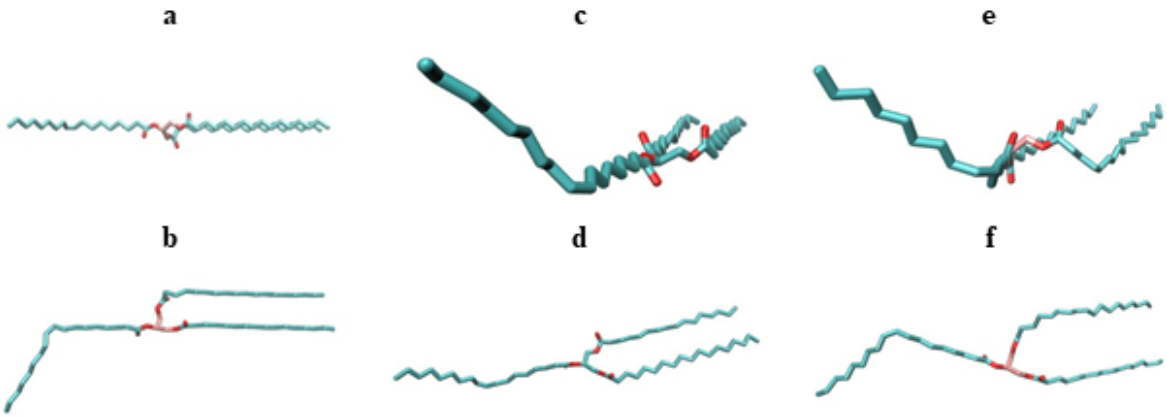

Figure 2. Visualization of a single *sn*-POSt molecule before equilibration (a and b) and after equilibration using GROMOS FF (c and d) and NERD FF (e and f) *(double column image)*

The shape of the molecule also changed on equilibration. Before equilibration the molecule was in a chair-like shape (even though technically it is in a tuning-fork conformation, *i.e.*, the oleic chain in the *sn*-2 position is positioned opposite to the other two chains), with the first part of the oleic chain (*i.e.*, before the *cis*-double bond) being in a straight line with the palmitic chain (Figure 2b). On equilibration, using the GROMOS FF, the chair-shape has a become a tuning-fork shape, with the glycerol ester linkage positions also being in a different conformation (Figure 2d), as also seen in the large difference of the angle formed by the ester oxygens when compared to the empirical structure (Table 1). On equilibration using the NERD FF the oleic chain is also no longer in line with the palmitic chain, however the ester linkage groups are in a conformation which is

much closer to the empirical structure (Figure 2f, Table 1), *i.e.*, the glycerol group conformation is retained much better.

Given these results, and in contrast to results obtained by Pizzirusso *et al*. where the NERD FF had reproduced the crystalline properties of fully saturated TAGs accurately,[6] neither of these two FFs were deemed to provide a satisfactory performance in reproducing the β_2 crystalline properties of the unsaturated TAG *sn*-POSt. However, given that the overall crystalline structure (dimensions and long spacing), and the glycerol-ester backbone, were better reproduced by the NERD FF, this FF was investigated further, and some modifications carried out.

The first change was to replace the Reaction Field electrostatics with PME electrostatics, however this still was not able to reproduce the crystalline properties accurately, with significant changes in the dimensions of the crystal (Table 2) and, more importantly, a change in the molecular conformation (Figure 3a). Further modifications were then carried out by varying the van der Waals (vdW) (fudgeLJ) and coulombic (fudgeQQ) fudge factors in GROMACS. The fudge factors fudgeLJ and fudgeQQ are used to scale the 1-4 Lennard-Jones (LJ) and coulombic (QQ) interactions respectively. Hence, a fudgeLJ factor of 0.5 scales down the 1-4 vdW interactions by half, with the scaling being applied to 1-4 coulombic interactions when using a fudgeQQ factor less than 1. Use of these fudge factors is not without precedent as other force fields do use fudge factors less than 1. Two such examples are the Amber99 force field, which uses fudgeLJ = 0.5 and fudgeQQ = 0.8333,[23] while the OPLS-AA forcefield uses fudgeLJ = fudgeQQ = 0.5.[24] A fudge factor sweep was thus carried out, with the results shown in Table 2.

Figure 3. Conformation of an *sn*-POSt molecule after equilibration using the modified NERD FF with PME electrostatics: (a) with fudgeLJ = fudgeQQ = 1; and (b) with fudgeLJ = 0.2 and fudgeQQ = 0.5 *(double column image)*

Measurements	Empirical[15]	NERD FF				
		coulomb = PME fudgeLJ = 1 fudgeQQ = 1	*coulomb = PME fudgeLJ = 0.5 fudgeQQ = 0.8333*	*coulomb = PME fudgeLJ = 0.5 fudgeQQ = 0.5*	*coulomb = PME fudgeLJ = 0.2 fudgeQQ = 0.5*	*coulomb = PME fudgeLJ = 0.05 fudgeQQ = 0.5*
a (Å)	27.12	25.13	25.16	25.40	25.49	26.04
b (Å)	126.53	134.43	132.95	132.79	131.85	131.21
c (Å)	40.605	41.98	41.83	41.71	41.48	40.95
α (°)	90.00	90.00	90.00	90.00	90.00	90.00
β (°)	88.51	88.66	88.66	88.64	88.63	88.58
γ (°)	90.00	90.00	90.00	90.00	90.00	90.00
Volume (Å^3)	139 336	141 770	138 974	140 631	139 356	138 810
Density (g/cm^3)	1.027	1.009	1.023	1.017	1.026	1.031
Long spacing (Å)	60.98	64.84	64.41	63.98	63.61	62.734
Glycerol backbone angle (°)	111.47	121.84	120.58	121.33	119.21	118.26
Ester oxygens angle (°)	66.65	61.47	61.71	62.09	61.98	63.18

Table 2. Comparison of empirical crystal properties of β_2 *sn*-POSt with simulated results using variations of the NERD FF.

From the results obtained it is clear that changing the vdW and electrostatic interactions has had an impact on the behavior of the crystal. A decrease in the fudge factor values resulted in a decrease in volume and corresponding increase in density, with the volume and density obtained when using PME electrostatics and fudgeLJ = 0.2 and fudgeQQ = 0.5 being near-identical to those found empirically. All the long spacing measurements were longer than those obtained by the unmodified NERD FF, however these were still considerably lower than that obtained when using the GROMOS FF (Table 1). The deviation in the angles formed by the glycerol backbone and the ester oxygens from the empirical value decreased with decreasing fudge factors, ostensibly due to the decreased intra-molecular repulsion.

Given the close packing of the atoms, which intra-molecularly are generally at distances around the energy minimum distance given by the LJ parameters, if the fudgeLJ factor is introduced, the attraction is reduced, but so is the repulsion if the atoms get too close due to natural movement/vibration, or are too close due to the crystalline structure. For example, the distance between the *sn*-1 glycerol CH_2 atom and the *sn*-3 ether oxygen in the crystal is 0.309 nm, however the LJ sigma value for the combined atoms is 0.3701, which results in repulsion. Hence if the LJ potentials are smaller due to a fudge factor less than 1 there will be less repulsion, and hence no distortion of the molecular conformation.

Changing the vdW and electrostatic interactions also had a major impact on the spatial conformation of the individual molecules. When using NERD FF the oleic chain was on a plane rotated by 47.8° to the palmitic-stearic chains plane (Table 3). On modifying the NERD FF the

rotation of the oleic chain decreased, although not to the degree observed in the near-equiplanar empirical configuration (Table 3). Visualisation of the individual molecules also showed an improvement in the shape of the molecule, with decreasing fudge factor values resulting in a shape closer to that found empirically, *i.e.*, with the palmitic chain in line with the first part of the oleic chain (Figure 3b).

Electrostatics	*fudgeLJ*	*fudgeQQ*	ε_{RF}	*Oleic chain plane rotation (°)*	σ (°)
Reaction-Field	1	1	2.975	47.8	11.2
PME	1	1	-	30.6	10.2
PME	0.5	0.833 3	-	24.0	4.0
PME	0.5	0.5	-	27.1	10.3
PME	0.2	0.5	-	23.0	7.1
PME	0.05	0.5	-	21.2	7.3

Table 3. Oleic chain plane rotation with respect to palmitic-stearic chains plane when using the (modified) NERD FF. The simulated values represent the average of triplicate equilibrations taken across all molecules in the simulation after equilibration had been reached. The standard deviations (σ) across the molecules and trajectories are provided.

Given these results, (i) a crystalline volume and density nearly equal to empirical; (ii) a much smaller deviation from empirical in the long spacing and the angle formed by ester oxygens, relative to the GROMOS results; and (iii) a molecular shape similar to empirical; it was thus determined that using the modified NERD FF, with PME electrostatics including fudgeLJ = 0.2 and fudgeQQ = 0.5, reproduced the β_2 *sn*-POSt crystal the best.

These force field parameters were then tested on the other main two TAGs which make up cocoa butter (*sn*-POP and *sn*-StOSt). The different temperatures used for the different equilibrations (see Supporting Information for simulation details) reflect the temperatures used for the respective empirical XRD measurements. In all cases the simulated density differed from the empirical value by less than 2%, with the individual dimensions differing by less than 6%. The α and γ angles of all the crystals remained at 90°, while the β angle deviated by less than 0.1% from the empirical value in all cases. In all cases the equilibrated long spacing was again longer than the empirical, however the equilibrated measurements differed from the empirical values by 5.3% or less (see Supporting Information - Table S1). Also, the molecular shape was maintained in all cases, *i.e.*, the molecules retained a chair-like shape with the first section of the oleic chain in line with the chain at the *sn*-1 position.

Determining the melted densities of *sn*-POSt, *sn*-POP and *sn*-StOSt yielded a linear relationship with temperature, with the density, as expected, decreasing with increasing temperature (Figure 4, Table S2). Interpolating for each TAG showed excellent agreement with empirical measurements (Table 4).

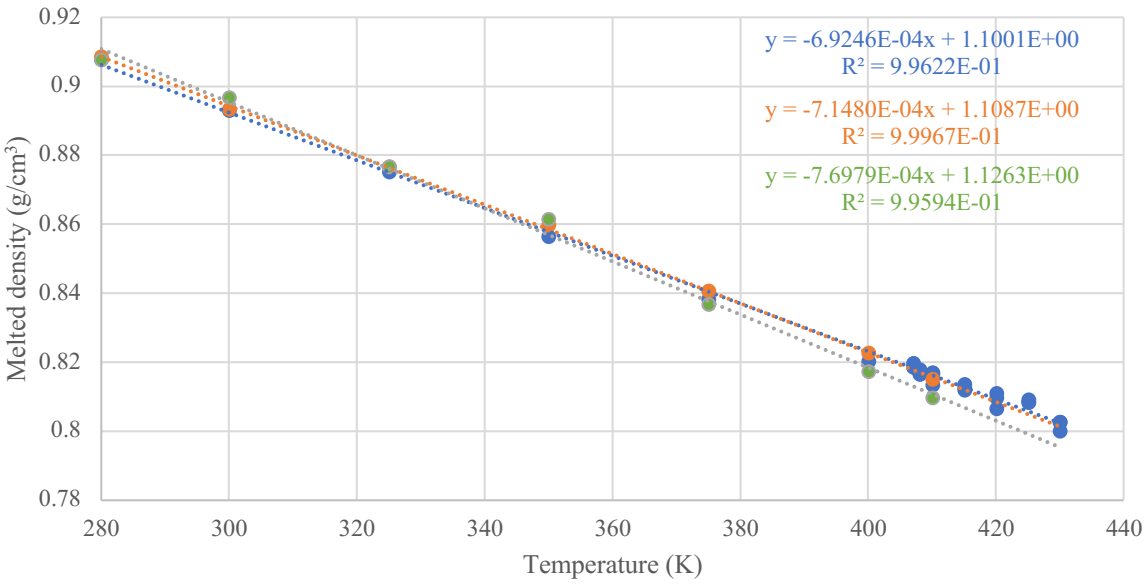

Figure 4. Plot of simulated melted density (g/cm^3) versus temperature (K) for *sn*-POSt (blue), *sn*-POP (orange) and *sn*-StOSt (green) (solid circles = simulated density measurements; broken line = best-fit line) *(1.5 column image)*

Temperature (K)		sn-*POSt*	sn-*POP*	sn-*StOSt*
293.15	Interpolated Simulated Density (g/cm^3)	0.897 1	0.899 2	0.900 7
	Empirical Density (g/cm^3)[25]	0.902 3	0.904 0	0.906 4
	% Difference from Empirical	-0.57%	-0.54%	-0.63%
313.15	Interpolated Simulated Density (g/cm^3)	0.883 3	0.884 9	0.885 3
	Empirical Density (g/cm^3)[25]	0.888 7	0.890 4	0.892 8
	% Difference from Empirical	-0.61%	-0.62%	-0.84%

Table 4. Interpolated simulated melted densities of the three major TAGs of cocoa butter and comparison with empirical values

CONCLUSIONS

Both the GROMOS96-53A5 and NERD (as described by Sum *et al*.[10]) force fields were found to be unsuitable to reproduce the correct molecular structure and crystalline density of the β_2 polymorph of the unsaturated TAG *sn*-POSt. Modification of the NERD FF, that is by using PME electrostatics and adjusting the fudgeLJ and fudgeQQ factors to 0.2 and 0.5 respectively, led to the macroscopic properties of the same TAG being reproduced much more accurately. The same modified force field was tested on the β_2 and β_1 polymorphs of *sn*-POSt, *sn*-POP and *sn*-StOSt, with the crystalline densities varying by less than 2% from the empirical values in all cases, while the crystalline dimensions varied by less than 6%. Comparison of the simulated melted densities of the same three TAGs also compared very well with empirical measurements, with a deviation of less than 1%.

With this modified FF the macroscopic crystalline and melted properties of unsaturated TAGs can thus be simulated, enabling the prediction of these properties for novel TAGs and fats.

ASSOCIATED CONTENT

Supporting Information

The Supporting Information is available free of charge at https://xxx

Comparison of equilibrated structures with empirical results, simulated densities and typical equilibration parameters (PDF)

Raw density results (.xvg text files)

Starting coordinates (.gro text files)

AUTHOR INFORMATION

Corresponding Author

Tell Tuttle – *Department of Pure and Applied Chemistry, University of Strathclyde, Glasgow G1 1XL, United Kingdom;* orcid.org/0000-0003-2300-8921; Email: tell.tuttle@strath.ac.uk

Author Contributions

The manuscript was written through contributions of all authors. All authors have given approval to the final version of the manuscript.

ACKNOWLEDGEMENT

The authors thank Mondelēz International for funding this work.

REFERENCES

(1) Chandrasekhar, I.; van Gunsteren, W. A Comparison of the Potential Energy Parameters of Aliphatic Alkanes: Molecular Dynamics Simulations of Triacylglycerols in the Alpha Phase. *Eur. Biophys. J.* **2002**, *31*, 89-101.

(2) Szewczyk, P. Study of the phase behavior of triacylglycerols using molecular dynamics simulation, University of Alberta, 2010.

(3) Brasiello, A.; Russo, L.; Siettos, C.; Milano, G.; Crescitelli, S. In *Multi-Scale Modelling And Coarse-Grained Analysis Of Triglycerides Dynamics;* Comput. Aided Chem. Eng.; 2010; Vol. 28, pp 625-630.

(4) MacDougall, C. J.; Razul, M. S.; Papp-Szabo, E.; Peyronel, F.; Hanna, C. B.; Marangoni, A. G.; Pink, D. A. Nanoscale Characteristics of Triacylglycerol Oils: Phase Separation and Binding Energies of Two-Component Oils to Crystalline Nanoplatelets. *Faraday Discuss*. **2012**, *158*, 425-433.

(5) Razul, M. S. G.; MacDougall, C. J.; Hanna, C. B.; Marangoni, A. G.; Peyronel, F.; Papp-Szabo, E.; Pink, D. A. Oil Binding Capacities of Triacylglycerol Crystalline Nanoplatelets: Nanoscale Models of Tristearin Solids in Liquid Triolein. *Food Funct* **2014**, *5*, 2501-2508.

(6) Pizzirusso, A.; Peyronel, F.; Co, E. D.; Marangoni, A. G.; Milano, G. Molecular Insights into the Eutectic Tripalmitin/Tristearin Binary System. *J. Am. Chem. Soc*. **2018**, *140*, 12405-12414.

(7) Noor Lida, H. M. D; Sundram, K.; Siew, W. L.; Aminah, A.; Mamot, S. TAG Composition and Solid Fat Content of Palm Oil, Sunflower Oil, and Palm Kernel Olein Belends before and After Chemical Interesterification. *J Am Oil Chem Soc* **2002**, *79*, 1137-1144.

(8) Parcerisa, J.; Codony, R.; Boatella, J.; Rafecas, M. Triacylglycerol and Phospholipid Composition of Hazelnut (Corylus avellanaL.) Lipid Fraction during Fruit Development. *J. Agric. Food Chem*. **1999**, *47*, 1410-1415.

(9) Alasalvar, C.; Shahidi, F.; Ohshima, T.; Wanasundara, U.; Yurttas, H. C.; Liyanapathirana, C. M.; Rodrigues, F. B. Turkish Tombul Hazelnut (Corylus avellanaL.). 2. Lipid Characteristics and Oxidative Stability. *J. Agric. Food Chem*. **2003**, *51*, 3797-3805.

(10) Sum, A. K.; Biddy, M. J.; de Pablo, J. J.; Tupy, M. J. Predictive Molecular Model for the Thermodynamic and Transport Properties of Triacylglycerols. *J. Phys. Chem. B* **2003**, *107*, 14443-14451.

(11) Greiner, M.; Elts, E.; Briesen, H. In *In Molecular Dynamics Simulations as a Predictive Tool for the Behavior of Fats in High-Pressure Processes;* 7th International Conference on Simulation and Modelling in the Food and Bio-Industry 2012, FOODSIM 2012; 2012; .

(12) Wang, J.; Wolf, R. M.; Caldwell, J. W.; Kollman, P. A.; Case, D. A. Development and Testing of a General Amber Force Field. *J Comput Chem* **2004**, *25*, 1157-1174.

(13) Beckett, S. T. In *The Science of Chocolate;* RSC paperbacks; Royal Society Of Chemistry: GB, 2008; .

(14) van Mechelen, J. B.; Peschar, R.; Schenk, H. Structures of Mono-unsaturated Triacylglycerols. I. the B1 Polymorph. *Acta. Crystallogr. B. Struct. Sci. Cryst. Eng. Mater*. **2006**, *62*, 1121-1130.

(15) Peschar, R.; Schenk, H.; van Mechelen, J. B. Structures of Mono-unsaturated Triacylglycerols. II. the B2 Polymorph. *Acta. Crystallogr. B. Struct. Sci. Cryst. Eng. Mater*. **2006**, *62*, 1131-1138.

(16) Martini, S.; Awad, T.; Marangoni, A. G. In *Structure and properties of fat crystal networks;* Gunstone, F. D., Ed.; Modifying Lipids for Use in Food; Woodhead Publishing: 2006; pp 142-169.

(17) Van Der Spoel, D.; Lindahl, E.; Hess, B.; Groenhof, G.; Mark, A. E.; Berendsen, H. J. C. GROMACS: Fast, Flexible, and Free. *J Comput Chem* **2005**, *26*, 1701-1718.

(18) Humphrey, W.; Dalke, A.; Schulten, K. VMD: Visual Molecular Dynamics. *J. Mol. Graph.* **1996**, *14*, 33-38.

(19) Oostenbrink, C.; Villa, A.; Mark, A. E.; van Gunsteren, W. F. A Biomolecular Force Field Based on the Free Enthalpy of Hydration and Solvation: The GROMOS Force-Field Parameter Sets 53A5 and 53A6. *J Comput Chem* **2004**, *25*, 1656-1676.

(20) Nath, S. K.; Escobedo, F. A.; de Pablo, J. J. On the Simulation of Vapor–liquid Equilibria for Alkanes. *J. Chem. Phys.* **1998**, *108*, 9905-9911.

(21) Nath, S. K.; Khare, R. New Forcefield Parameters for Branched Hydrocarbons. *J. Chem. Phys.* **2001**, *115*, 10837-10844.

(22) Nath, S. K.; Banaszak, B. J.; de Pablo, J. J. A New United Atom Force Field for A-Olefins. *J. Chem. Phys.* **2001**, *114*, 3612-3616.

(23) Sorin, E. J.; Pande, V. S. Exploring the Helix-Coil Transition Via all-Atom Equilibrium Ensemble Simulations. *Biophys. J.* **2005**, *88*, 2472-2493.

(24) Jorgensen, W. L.; Maxwell, D. S.; Tirado-Rives, J. Development and Testing of the OPLS all-Atom Force Field on Conformational Energetics and Properties of Organic Liquids. *J. Am. Chem. Soc.* **1996**, *118*, 11225-11236.

(25) Arishima, T.; Sagi, N.; Mori, H.; Sato, K. Density Measurement of the Polymorphic Forms of POP, POS and SOS. *J. Japan Oil Chem. Soc.* **1995**, *44*, 431-437.